Equivalent Linearization Analysis of Geometrically Nonlinear Random Vibrations Using Commercial Finite Element Codes

Stephen A. Rizzi and Alexander A. Muravyov
Langley Research Center, Hampton, Virginia

The NASA STI Program Office . . . in Profile

Since its founding, NASA has been dedicated to the advancement of aeronautics and space science. The NASA Scientific and Technical Information (STI) Program Office plays a key part in helping NASA maintain this important role.

The NASA STI Program Office is operated by Langley Research Center, the lead center for NASA's scientific and technical information. The NASA STI Program Office provides access to the NASA STI Database, the largest collection of aeronautical and space science STI in the world. The Program Office is also NASA's institutional mechanism for disseminating the results of its research and development activities. These results are published by NASA in the NASA STI Report Series, which includes the following report types:

- TECHNICAL PUBLICATION. Reports of completed research or a major significant phase of research that present the results of NASA programs and include extensive data or theoretical analysis. Includes compilations of significant scientific and technical data and information deemed to be of continuing reference value. NASA counterpart of peer-reviewed formal professional papers, but having less stringent limitations on manuscript length and extent of graphic presentations.

- TECHNICAL MEMORANDUM. Scientific and technical findings that are preliminary or of specialized interest, e.g., quick release reports, working papers, and bibliographies that contain minimal annotation. Does not contain extensive analysis.

- CONTRACTOR REPORT. Scientific and technical findings by NASA-sponsored contractors and grantees.

- CONFERENCE PUBLICATION. Collected papers from scientific and technical conferences, symposia, seminars, or other meetings sponsored or co-sponsored by NASA.

- SPECIAL PUBLICATION. Scientific, technical, or historical information from NASA programs, projects, and missions, often concerned with subjects having substantial public interest.

TECHNICAL TRANSLATION. English-language translations of foreign scientific and technical material pertinent to NASA's mission.

Specialized services that complement the STI Program Office's diverse offerings include creating custom thesauri, building customized databases, organizing and publishing research results . . . even providing videos.

For more information about the NASA STI Program Office, see the following:

- Access the NASA STI Program Home Page at *http://www.sti.nasa.gov*

- Email your question via the Internet to help@sti.nasa.gov

- Fax your question to the NASA STI Help Desk at (301) 621-0134

- Telephone the NASA STI Help Desk at (301) 621-0390

- Write to:
  NASA STI Help Desk
  NASA Center for AeroSpace Information
  7121 Standard Drive
  Hanover, MD 21076-1320

NASA/TP-2002-211761

Equivalent Linearization Analysis of Geometrically Nonlinear Random Vibrations Using Commercial Finite Element Codes

Stephen A. Rizzi and Alexander A. Muravyov
Langley Research Center, Hampton, Virginia

July 2002

ABSTRACT

Two new equivalent linearization implementations for geometrically nonlinear random vibrations are presented. Both implementations are based upon a novel approach for evaluating the nonlinear stiffness within commercial finite element codes and are suitable for use with any finite element code having geometrically nonlinear static analysis capabilities. The formulation includes a traditional force-error minimization approach and a relatively new version of a potential energy-error minimization approach, which has been generalized for multiple degree-of-freedom systems. Results for a simply supported plate under random acoustic excitation are presented and comparisons of the displacement root-mean-square values and power spectral densities are made with results from a nonlinear time domain numerical simulation.

1. INTRODUCTION

Current efforts to extend the performance and flight envelope of high-speed aerospace vehicles have resulted in structures which may respond to the imposed dynamic loads in a geometrically nonlinear (large deflection) random fashion. What differentiates the geometrically nonlinear random response considered in this paper from a linear response is the presence of bending-membrane coupling, which gives rise to membrane stretching (in-plane stresses) in the former. This coupling has the effect of stiffening the structure and reducing the dynamic response relative to that of the linear system. Linear analyses do not account for this effect and consequently may significantly over-predict the response, leading to grossly conservative designs. Without practical design tools capable of capturing the nonlinear dynamics, further improvements in vehicle performance and system design will be hampered.

Methods currently used to predict geometrically nonlinear random response include perturbation, Fokker-Plank-Kolmogorov (F-P-K), numerical simulation and stochastic linearization techniques. All have various limitations. Perturbation techniques are limited to weak geometric nonlinearities. The F-P-K approach [1, 2] yields exact solutions, but can only be applied to simple mechanical systems. Numerical simulation techniques using numerical integration provide time histories of the response from which statistics of the random response may be calculated. This, however, comes at a high computational expense due to the long time records or high number of ensemble averages required to get high quality random response statistics. Statistical linearization methods, for example equivalent linearization (EL) [[2-7]), have seen the

broadest application because of their ability to accurately capture the response statistics over a wide range of response levels while maintaining relatively light computational burden. In EL methods, an equivalent linear system is sought such that the difference between the equivalent linear and nonlinear systems is minimized. Traditionally, the difference between the nonlinear force and the product of the equivalent linear stiffness and displacement response vector is minimized.

Since the analysis of complicated structural geometries is required, a finite element-based EL method is considered most appropriate. In the past, implementations of EL using finite element analysis have been limited to special purpose codes. This is largely due to the inaccessibility of the nonlinear element formulation in commercial finite element applications. For example, the nonlinear stiffness of a rectangular plate finite element was found in [8] after a lengthy analytical derivation, which utilized information about the element shape functions.

The first known EL implementation in a general-purpose finite element code [9] was developed for use in MSC.NASTRAN [10] version 67. In that implementation, called "Super Element Modal Equivalent Linear Random Response" or SEMELRR, the equivalent linear stiffness was obtained as the sum of the linear stiffness and three times the differential stiffness. While this form was convenient to implement, it was found to over-predict the degree of nonlinearity and produce non-conservative results. Over-prediction of nonlinearity can produce the undesirable result of structural designs incapable of withstanding the applied loads in an acceptable fashion.

This paper describes a novel approach to accurately determine the nonlinear stiffness without using a description of the element shape functions [11, 12]. The approach solves a series of inverse linear and nonlinear static problems to evaluate the nonlinear force, from which the nonlinear stiffness can be determined. While it is applicable to any commercial finite element program having a nonlinear static analysis capability, MSC.NASTRAN was selected due to its widespread use in the aerospace industry. The stiffness evaluation technique was first validated for a beam structure under a special loading condition [12]. More recently, it was validated for a clamped-clamped beam under random inertial loading through comparison with a finite element-based numerical simulation analysis in physical coordinates [13].

In addition, this paper describes the generalization of a relatively new potential energy-error minimization version of the EL method [6, 7] to a multiple degree-of-freedom case. This new minimization approach was previously validated using the F-P-K method for a few special cases including a Duffing oscillator and a two degree-of-freedom system [11] and for a beam structure [12].

To further validate the nonlinear stiffness evaluation approach and its use in an EL analysis using force-error and potential energy-error minimization, a simply supported plate subjected to random acoustic loading is considered. This case is also closely related to the intended application. Results are compared with a finite element-based numerical simulation analysis in modal coordinates, as described in [14]. The numerical simulation analysis in modal coordinates was selected for this purpose because the solution in physical coordinates was intractable due to the large system size. The use of a modal approach is considered acceptable for the class of problems exhibiting bending-membrane coupling, as in the simply supported plate.

2. NONLINEAR STIFFNESS EVALUATION

The equations of motion of a multiple degree-of-freedom, viscously damped geometrically nonlinear system can be written in the form:

$$M\ddot{X}(t) + C\dot{X}(t) + KX(t) + \Gamma(X(t)) = F(t) \tag{1}$$

where M, C, K are the mass, damping, and stiffness matrices, X is the displacement response vector and F is the force excitation vector, respectively. The nonlinear force term $\Gamma(X)$ is a vector function, which generally includes second and third order terms in X.

Solution to equation (1) via any method requires knowledge of the system matrices. In the context of a commercial finite element program, M, C, and K are generally available. In the EL analyses to follow, the nonlinear stiffness is required. The nonlinear stiffness is related to Γ, which is typically not available within a commercial finite element program. Therefore, a means of numerically evaluating Γ was developed, as is next described, for the determination of the nonlinear stiffness.

A set of coupled modal equations with reduced degrees-of-freedom is first obtained by applying the modal coordinate transformation

$$X = \Phi q \tag{2}$$

3

to equation (1), where Φ is generally a subset ($L \leq N$) of the linear eigenvectors , $\boldsymbol{q}$ is the vector of modal coordinates, and the time dependence is implied. This coupled set is expressed as

$$\tilde{\boldsymbol{M}}\ddot{\boldsymbol{q}} + \tilde{\boldsymbol{C}}\dot{\boldsymbol{q}} + \tilde{\boldsymbol{K}}\boldsymbol{q} + \gamma(q_1, q_2, \ldots, q_L) = \tilde{\boldsymbol{F}} \tag{3}$$

where

$$\tilde{\boldsymbol{M}} = \Phi^T \boldsymbol{M} \Phi = \lceil \boldsymbol{I} \rfloor$$
$$\tilde{\boldsymbol{C}} = \Phi^T \boldsymbol{C} \Phi = \lceil 2\zeta_r \omega_r \rfloor$$
$$\tilde{\boldsymbol{K}} = \Phi^T \boldsymbol{K} \Phi = \lceil \omega_r^2 \rfloor$$
$$\gamma = \Phi^T \Theta$$
$$\tilde{\boldsymbol{F}} = \Phi^T \boldsymbol{F}$$

$q_1, q_2, \ldots, q_L$ are the components of $\boldsymbol{q}$, and ω_r are the undamped natural frequencies. The components of the nonlinear force vector may be written in the form

$$\gamma_r(q_1, q_2, \ldots, q_L) = \sum_{j=1}^{L}\sum_{k=j}^{L} a_{jk}^r q_j q_k + \sum_{j=1}^{L}\sum_{k=j}^{L}\sum_{l=k}^{L} b_{jkl}^r q_j q_k q_l \qquad r = 1, 2, \ldots, L \,. \tag{4}$$

where a_{jk}^r and b_{jkl}^r are nonlinear stiffness coefficients with $j = 1, 2, \ldots, L$, $k = j, j+1, \ldots, L$ and $l = k, k+1, \ldots, L$. This particular form of γ facilitates the subsequent solution of the equivalent linear system. Its evaluation entails solving for the coefficients a_{jk} and b_{jkl} using a new procedure developed for use with finite element programs having a nonlinear static solution capability.

The procedure is based on the restoration of nodal applied forces by prescribing nodal displacements to both linear and nonlinear static solutions. The total nodal force $\boldsymbol{F}_T$ may be written in physical coordinates as

$$\boldsymbol{F}_T = \boldsymbol{F}_L + \boldsymbol{F}_{NL} = \boldsymbol{K}\boldsymbol{X}_c + \Theta(\boldsymbol{X}_c) \tag{5}$$

where $\boldsymbol{X}_c$ is a prescribed physical nodal displacement vector, and $\boldsymbol{F}_L$ and $\boldsymbol{F}_{NL}$ are the linear and nonlinear contributions to the total nodal force. $\boldsymbol{F}_L$ is first obtained by prescribing $\boldsymbol{X}_c$ in the linear static solution. $\boldsymbol{F}_T$ is then obtained by prescribing $\boldsymbol{X}_c$ in the nonlinear static solution which includes both linear and nonlinear contributions. Finally, the nonlinear contribution $\boldsymbol{F}_{NL}$ is obtained by subtracting $\boldsymbol{F}_L$ from $\boldsymbol{F}_T$, or

$$F_{NL} \equiv (X_c) \equiv F_T - F_L \,. \tag{6}$$

To illustrate the technique, one can begin by prescribing the displacement fields

$$X_c = \phi_1 q_1$$
$$X_c = -\phi_1 q_1$$

The nonlinear nodal force contributions F_{NL} are determined using (6) after solving the linear and nonlinear static solutions. These may be written in modal coordinates as

$$F_{NL_1} = {}^T F_{NL_1} = {}^T (\phi_1 q_1) = \left[a_{11}^r\right] q_1 q_1 + \left[b_{111}^r\right] q_1 q_1 q_1$$
$$F_{NL_2} = {}^T F_{NL_2} = {}^T (-\phi_1 q_1) = \left[a_{11}^r\right] q_1 q_1 - \left[b_{111}^r\right] q_1 q_1 q_1 \tag{7}$$

where the sought stiffness coefficients $[a_{11}^r]$ and $[b_{111}^r]$ are column vectors of length L. Note that the other nonlinear terms do not appear in (7) since $q_j = 0$ for $j \neq 1$. Since q_1 is a known scalar, the coefficients $[a_{11}^r]$ and $[b_{111}^r]$ for $r = 1,2,\ ,L$ can be determined from the resulting system (7) of $2 \times L$ linear equations. The remaining coefficients $[a_{jj}^r]$ and $[b_{jjj}^r]$ ($j = 2,3\ ,L$) can be determined in an analogous manner.

A similar technique can be employed to determine stiffness coefficients with two unequal lower indices, e.g., $[a_{12}^r]$, $[b_{112}^r]$, and $[b_{122}^r]$. Coefficients of this type appear only if the number of retained eigenvectors is greater than or equal to two ($L \geq 2$). Prescribing the displacement fields

$$X_c = \phi_1 q_1 + \phi_2 q_2$$
$$X_c = -\phi_1 q_1 - \phi_2 q_2$$
$$X_c = \phi_1 q_1 - \phi_2 q_2$$

results in the following equations

$$F_{NL_1} = \Phi^T \left(\Phi_1 q_1 + \Phi_2 q_2 \right) = \left[a_{11}^r \right] q_1 q_1 + \left[b_{111}^r \right] q_1 q_1 q_1 + \left[a_{22}^r \right] q_2 q_2 + \left[b_{222}^r \right] q_2 q_2 q_2$$
$$+ \left[a_{12}^r \right] q_1 q_2 + \left[b_{112}^r \right] q_1 q_1 q_2 + \left[b_{122}^r \right] q_1 q_2 q_2$$

$$F_{NL_2} = \Phi^T \left(-\Phi_1 q_1 + \Phi_2 q_2 \right) = \left[a_{11}^r \right] q_1 q_1 - \left[b_{111}^r \right] q_1 q_1 q_1 + \left[a_{22}^r \right] q_2 q_2 + \left[b_{222}^r \right] q_2 q_2 q_2 \qquad (8)$$
$$- \left[a_{12}^r \right] q_1 q_2 - \left[b_{112}^r \right] q_1 q_1 q_2 + \left[b_{122}^r \right] q_1 q_2 q_2$$

$$F_{NL_3} = \Phi^T \left(\Phi_1 q_1 - \Phi_2 q_2 \right) = \left[a_{11}^r \right] q_1 q_1 + \left[b_{111}^r \right] q_1 q_1 q_1 + \left[a_{22}^r \right] q_2 q_2 - \left[b_{222}^r \right] q_2 q_2 q_2$$
$$- \left[a_{12}^r \right] q_1 q_2 + \left[b_{112}^r \right] q_1 q_1 q_2 - \left[b_{122}^r \right] q_1 q_2 q_2$$

Summing the first two of equations (8) results in

$$F_{NL_1} + F_{NL_2} = 2 \left[a_{11}^r \right] q_1 q_1 + 2 \left[a_{22}^r \right] q_2 q_2 + 2 \left[a_{12}^r \right] q_1 q_2$$

from which the coefficients $[a_{12}^r]$ may be determined, since $[a_{11}^r]$ and $[a_{22}^r]$ were previously determined. Then, from the first and third of equations (8), the coefficients $[b_{112}^r]$ and $[b_{122}^r]$ may be determined from the $2 \times L$ system of equations. In this manner, all coefficients of the type $[b_{jjk}^r]$ and $[b_{kkj}^r]$ for $j, k = 1, 2, \dots, L$ may be determined.

For cases when the number of retained eigenvectors is greater than or equal to three ($L \geq 3$), coefficients with three unequal lower indices, e.g., $[b_{123}^r]$, may be determined by prescribing the displacement field

$$X_c = \Phi_1 q_1 + \Phi_2 q_2 + \Phi_3 q_3 .$$

The resulting equation

$$F_{NL} = \Phi^T \left(\Phi_1 q_1 + \Phi_2 q_2 + \Phi_3 q_3 \right)$$
$$= \left[a_{11}^r \right] q_1 q_1 + \left[a_{22}^r \right] q_2 q_2 + \left[a_{33}^r \right] q_3 q_3 + \left[a_{12}^r \right] q_1 q_2 + \left[a_{13}^r \right] q_1 q_3 + \left[a_{23}^r \right] q_2 q_3$$
$$+ \left[b_{111}^r \right] q_1 q_1 q_1 + \left[b_{222}^r \right] q_2 q_2 q_2 + \left[b_{333}^r \right] q_3 q_3 q_3 + \left[b_{112}^r \right] q_1 q_1 q_2 + \left[b_{221}^r \right] q_2 q_2 q_1 \qquad (9)$$
$$+ \left[b_{113}^r \right] q_1 q_1 q_3 + \left[b_{331}^r \right] q_3 q_3 q_1 + \left[b_{223}^r \right] q_2 q_2 q_3 + \left[b_{332}^r \right] q_3 q_3 q_2 + \left[b_{123}^r \right] q_1 q_2 q_3$$

contains one column of unknown coefficients $[b_{123}^r]$. All coefficients of type $[b_{jkl}^r]$ ($j \neq k \neq l$) can be found in this manner.

Having the modal equations of motion (3) formulated, their solution can be undertaken through a variety of techniques. For the reasons previously discussed, application of EL is considered.

3. EQUIVALENT LINEARIZATION APPROACH

An approximate solution to (1) can be achieved by formation of an equivalent linear system:

$$M\ddot{X}(t) + C\dot{X}(t) + (K + K_e)X(t) = F(t) \tag{10}$$

where K_e is the equivalent linear stiffness matrix. While it is possible to perform an EL analysis in the physical degrees-of-freedom, it is desirable to recast the problem in modal coordinates to simplify the problem. The equivalent linear analog of equation (3) may be found by applying the modal transformation (2) to (10):

$$M\ddot{q} + C\dot{q} + [K + \overline{K}_e]q = \overline{F} \tag{11}$$

where the fully populated modal equivalent stiffness matrix is given by

$$\overline{K}_e = \Phi^T K_e \Phi \quad .$$

Two EL approaches are considered. One is based on minimization of the error in the nonlinear force vector and the other minimizes the error in potential (strain) energy.

3.1. FORCE-ERROR MINIMIZATION APPROACH

The traditional (force-error minimization) method of EL seeks to minimize the difference between the nonlinear force and the product of the equivalent linear stiffness and displacement response vector. Since the error is a random function of time, the required condition is that the expectation of the mean square error be a minimum [3], i.e.

$$error = E\left\{(\Theta(X) - K_e X)^T(\Theta(X) - K_e X)\right\} \rightarrow \min \tag{12}$$

where $E[\dots]$ represents the expectation operator. Equation (12) will be satisfied if

$$\frac{\partial(error)}{\partial K_{eij}} = 0 \qquad i,j = 1,2, \dots ,N$$

where K_{eij} are the elements of matrix K_e, and N is the number of physical degrees of freedom. In this study, consideration is limited to the case of Gaussian, zero-mean excitation and response to simplify the solution. With these assumptions and omitting intermediate derivations, the final form for the equivalent linear stiffness matrix in physical coordinates becomes (see for example [4], [5]):

$$\boldsymbol{K}_e = \left[E\left[\frac{\partial}{\partial \boldsymbol{X}} \right] \right] \tag{13}$$

and in modal coordinates becomes

$$\boldsymbol{K}_e = \left[E\left[\frac{\partial}{\partial \boldsymbol{q}} \right] \right] \tag{14}$$

with $\Box$ as previously defined in (4).

3.2. POTENTIAL ENERGY-ERROR MINIMIZATION APPROACH

An alternative EL approach based on potential (strain) energy-error minimization was proposed in [6, 7]. Analysis in these works was limited to single degree-of-freedom systems and simplified multiple degree-of-freedom systems. In this study, that approach is rigorously generalized for the case of coupled multiple degree-of-freedom systems. One can begin with an expression for the error in potential energy

$$error = E\left[\left(U(\boldsymbol{X}) - \tfrac{1}{2} \boldsymbol{X}^T \boldsymbol{K}_e \boldsymbol{X} \right)^2 \right] \tag{15}$$

where $U(\boldsymbol{X})$ is the potential energy of the original (nonlinear) system. A condition of minimized error requires that

$$E\left[\frac{\partial}{\partial K_{eij}} \left(U(\boldsymbol{X}) - \tfrac{1}{2} \boldsymbol{X}^T \boldsymbol{K}_e \boldsymbol{X} \right)^2 \right] = 0 \qquad i,j = 1,2, \dots, N. \tag{16}$$

Omitting intermediate derivations, one obtains the following system of N^2 linear equations with respect to unknown elements of matrix $\boldsymbol{K}_e$:

$$\sum_{i=1}^{N} \sum_{j=1}^{N} K_{eij} E\left[x_i x_j x_k x_l \right] = 2E\left[x_k x_l U(\boldsymbol{X}) \right] \qquad k,l = 1,2, \dots, N. \tag{17}$$

For example, equation (17) would have the following form for a two degree-of-freedom system

$$
\begin{bmatrix}
E\{x_1^4\} & E\{x_1^3 x_2\} & E\{x_1^3 x_2\} & E\{x_1^2 x_2^2\} \\
E\{x_1^3 x_2\} & E\{x_1^2 x_2^2\} & E\{x_1^2 x_2^2\} & E\{x_1 x_2^3\} \\
E\{x_1^3 x_2\} & E\{x_1^2 x_2^2\} & E\{x_1^2 x_2^2\} & E\{x_1 x_2^3\} \\
E\{x_1^2 x_2^2\} & E\{x_1 x_2^3\} & E\{x_1 x_2^3\} & E\{x_2^4\}
\end{bmatrix}
\begin{Bmatrix}
K_{e11} \\ K_{e12} \\ K_{e21} \\ K_{e22}
\end{Bmatrix}
= 2
\begin{Bmatrix}
E\{x_1^2 U(X)\} \\
E\{x_1 x_2 U(X)\} \\
E\{x_1 x_2 U(X)\} \\
E\{x_2^2 U(X)\}
\end{Bmatrix}
\tag{18}
$$

This system of equations is under-determined (the second and third rows are identical), so an additional equation is required to solve this system. The additional equation(s) can be provided by imposing symmetry of the matrix $\boldsymbol{K}_e$, i.e., $K_{eij} = K_{eji}$.

Note that the formulation for the multiple degree-of-freedom system in reference [7] differs from the above formulation. The multiple degree-of-freedom case in [7] is treated by introduction of only diagonal terms of the matrix $\boldsymbol{K}_e$, whereas in this study the complete matrix $\boldsymbol{K}_e$ is formulated and is thereby advantageous in cases which exhibit modal coupling.

In modal coordinates, the equivalent linear stiffness matrix is related to nonlinear stiffness terms in a more complicated manner than in the force-error minimization approach. It is known that the nonlinear elastic force terms satisfy the following

$$
\gamma_r(q_1, q_2, \ldots, q_L) = \frac{\partial U}{\partial q_r} \qquad r = 1, 2, \ldots, L
\tag{19}
$$

where U is the potential energy generated by nonlinear terms only. The potential energy of the system may be written in the following form

$$
U = \sum_{s=1}^{L} \sum_{j=s}^{L} \sum_{k=j}^{L} \sum_{l=k}^{L} d_{sjkl} q_s q_j q_k q_l
\tag{20}
$$

which upon substitution into (19) yields

$$
\gamma_r(q_1, q_2, \ldots, q_L) = \frac{\partial}{\partial q_r}\left(\sum_{s=1}^{L} \sum_{j=s}^{L} \sum_{k=j}^{L} \sum_{l=k}^{L} d_{sjkl} q_s q_j q_k q_l \right).
\tag{21}
$$

The coefficients d_{sjkl} are related to the nonlinear stiffness coefficients through equation (4) as:

$$
\sum_{j=1}^{L} \sum_{k=j}^{L} a_{jk}^r q_j q_k + \sum_{j=1}^{L} \sum_{k=j}^{L} \sum_{l=k}^{L} b_{jkl}^r q_j q_k q_l = \frac{\partial}{\partial q_r}\left(\sum_{s=1}^{L} \sum_{j=s}^{L} \sum_{k=j}^{L} \sum_{l=k}^{L} d_{sjkl} q_s q_j q_k q_l \right)
\tag{22}
$$

In the following, a zero-mean response is assumed, i.e., $E[\boldsymbol{q}] = 0$. As will be subsequently shown, this has the effect of dropping out the quadratic terms a_{jk}. From (22), the coefficients d_{sjkl} can then be written as:

$$d_{sjkl} = \begin{cases} b^s_{jkl}/2 & s = j \\ b^s_{jkl}/3 & s = j = k \\ b^s_{jkl}/4 & s = j = k = l \\ b^s_{jkl} & \text{otherwise.} \end{cases} \tag{23}$$

Note that if the zero-mean response assumption were not made, the above relationship would be more complicated. Having U now fully defined from equation (20), the modal equivalent of equation (17) can be written as

$$\sum_{i=1}^{L} \sum_{j=1}^{L} K_{eij} E\left[q_i q_j q_k q_l \right] = 2 E\left[q_k q_l U(\boldsymbol{q}) \right] \qquad k,l = 1,2, \ldots ,L \tag{24}$$

from which $\boldsymbol{K}_e$ can be determined. The matrix on the left hand side of equation (24) involves 4th order moments of modal displacements. The right hand side involves 4th, 5th and 6th order modal displacement moments since the potential energy is a function of the 2nd, 3rd, and 4th order displacements. Assuming a Gaussian distributed, zero-mean response, the odd order moments are zero and the higher order even moments can be expressed in terms of the 2nd order moments. For example,

$$E\left[q_i q_j q_k q_l \right] = E\left[q_i q_j \right] E\left[q_k q_l \right] + E\left[q_i q_k \right] E\left[q_j q_l \right] + E\left[q_i q_l \right] E\left[q_j q_k \right].$$

Therefore, the matrices of equation (24) can be written solely in terms of the modal response covariance.

4. ITERATIVE SOLUTION

Because the modal equivalent linear stiffness matrix $\boldsymbol{K}_e$ is a function of the unknown modal displacements, the solution takes an iterative form. The time variation of the modal displacements and forces may be expressed as:

$$\boldsymbol{q}(t) = \sum_{n} \hat{\boldsymbol{q}} e^{i\Omega_n t} \qquad \boldsymbol{f}(t) = \sum_{n} \hat{\boldsymbol{f}} e^{i\Omega_n t} \tag{25}$$

where (^) indicates the dependency on ω_n. Applying (25) to (11) and writing in iterative form gives:

$$\hat{q}^m = H^{m-1}\hat{f} \qquad (26)$$

where m is the iteration number and

$$H^{m-1} = \left[-\omega_n^2 M + i\omega_n C + K + [\alpha K_e^{m-1} + \beta K_e^{m-2}] \right]^{-1} \qquad (27)$$

The introduction of the weightings α and β are to aid in the convergence of the solution, with the condition that $\alpha + \beta = 1$.

For stochastic excitation, (26) is rewritten as:

$$S_q^m = H^{m-1} S_f \left[\bar{H}^{m-1} \right]^T \qquad (28)$$

and the r,s component of the covariance matrix of modal displacements is

$$E[q_r q_s]^m = \sum_n S_{q_r q_s}^m \Delta \omega_n$$

Here, S_q is the spectral density matrix of modal displacements and S_f is the spectral density matrix of the load in modal coordinates. The diagonal elements, $S_{q_r q_r}$, are the variances of the modal displacements. K_e is zero for the first iteration, which yields the covariance matrix $E[q_r q_s]$ of the linear system. For subsequent iterations ($m>1$), the nonlinear stiffness depends on the minimization approach taken.

For example, for the force-error minimization approach, K_e for the mth iteration is determined from (14) as

$$K_e^m = \left[E\left\{ \frac{\partial \theta}{\partial q} \right\} \right]^m = \begin{bmatrix} E\left\{ \frac{\partial \theta_1}{\partial q_1} \right\} & \cdots & E\left\{ \frac{\partial \theta_1}{\partial q_L} \right\} \\ \vdots & \ddots & \vdots \\ E\left\{ \frac{\partial \theta_L}{\partial q_1} \right\} & \cdots & E\left\{ \frac{\partial \theta_L}{\partial q_L} \right\} \end{bmatrix}^m \qquad (29)$$

Substitution of equation (4) into (29) gives

$$K_e^m = \begin{bmatrix} \sum_j^L a_{j1}^1 E[q_j] + \sum_{j=1}^L \sum_{k\neq j}^L b_{jk1}^1 E[q_j q_k] & \cdots & \sum_j^L a_{jL}^1 E[q_j] + \sum_{j=1}^L \sum_{k\neq j}^L b_{jkL}^1 E[q_j q_k] \\ \vdots & & \vdots \\ \sum_j^L a_{j1}^L E[q_j] + \sum_{j=1}^L \sum_{k\neq j}^L b_{jk1}^L E[q_j q_k] & \cdots & \sum_j^L a_{jL}^L E[q_j] + \sum_{j=1}^L \sum_{k\neq j}^L b_{jkL}^L E[q_j q_k] \end{bmatrix}^{m-1} \tag{30}$$

Since a zero-mean response is assumed, i.e. $E[q] = 0$, equation (30) reduces to:

$$K_e^m = \begin{bmatrix} \sum_{j=1}^L \sum_{k\neq j}^L b_{jk1}^1 E[q_j q_k] & \cdots & \sum_{j=1}^L \sum_{k\neq j}^L b_{jkL}^1 E[q_j q_k] \\ \vdots & & \vdots \\ \sum_{j=1}^L \sum_{k\neq j}^L b_{jk1}^L E[q_j q_k] & \cdots & \sum_{j=1}^L \sum_{k\neq j}^L b_{jkL}^L E[q_j q_k] \end{bmatrix}^{m-1} \tag{31}$$

For the potential energy-error minimization approach, K_e is found by solving the system of equations (24) in a similar iterative fashion.

For both error minimization approaches, the iterations continue until convergence of the modal equivalent linear stiffness matrix such that

$$\left\| K_e^m - K_e^{m-1} \right\| < \varepsilon$$

The value of ε typically used is 0.1%.

Following convergence, the $N \times N$ covariance matrix of the displacements in physical coordinates is recovered from

$$E\{x_i x_j\} = \Phi \, E[q_r q_s] \, \Phi^T \tag{32}$$

and root-mean-square (RMS) values are the square roots of the diagonal terms in (32). Further post-processing to obtain power spectral densities of displacements, stresses, strains, etc., may be performed by substituting the converged equivalent stiffness matrix into (11) and solving in the usual linear fashion.

5. IMPLEMENTATION

The EL procedures as outlined above were recently implemented within the context of MSC.NASTRAN [10] version 70.0 (heretofore NASTRAN) using the DMAP programming language [15]. Its operation has been verified through NASTRAN version 70.7. Details of these

implementations, collectively called ELSTEP for "Equivalent Linearization using a STiffness Evaluation Procedure," are documented in [16]. The implementations entail first performing a normal modes analysis (solution 103) to obtain the modal matrices, from which a subset of L modes are chosen. The nonlinear stiffness coefficients are then determined by performing a series of linear static (solution 101) and nonlinear static (solution 106) solutions using linear combinations of modes as previously described. The iterative solution is performed in a standalone routine, which has as its output the RMS displacements in physical coordinates, the cross covariance in modal coordinates, and the sum of the linear and equivalent linear modal stiffness matrices. The latter can then be substituted for the linear modal stiffness in the modal frequency response analysis (solution 111) for post-processing.

6. NUMERICAL SIMULATION ANALYSIS

For validation purposes, a numerical simulation analysis was performed to generate time history results from which response statistics could be calculated. The particular method used was finite element-based with the integration performed in modal coordinates, as described in [14]. The finite element model uses the 4-node, Bogner-Fox-Schmit (BFS) C^1 conforming rectangular element with 24 degrees-of-freedom: 4 bending degrees-of-freedom ($w, \partial w/\partial x, \partial w/\partial y, \partial^2 w/\partial x \partial y$) and 2 in-plane degrees-of-freedom (u, v) at each node. The equations of motion are derived using the von Karman large deformation theory. In applying this modal approach, the modal truncation should be the same as that used in the EL approach.

6.1. LOADING TIME HISTORY AND TRANSIENT RESPONSE PROCESSING

The time history of the load was generated as described in [14]. A time increment (Δt) of 122 μs was found suitable for the numerical integration and time history records of 2.0 s in duration were generated using a record length of 2^{14} samples. A radix-2 number of samples was chosen to facilitate use of radix-2 FFT algorithms employed for the subsequent analysis. An ensemble of time histories was generated by specifying different seeds to the random number generator.

A typical time history corresponding to a pressure load of 8 Pa RMS (112 dB) is shown in Figure 1. The corresponding probability density function is shown in Figure 2 with the Gaussian distribution superimposed upon it. The power spectral density (PSD) for 10 ensemble averages gives a spectrum level of 6.25×10^{-2} Pa^2/Hz over a 1024 Hz bandwidth as shown Figure 3. A

sharp roll-off of the input spectrum practically eliminates excitation of the structure outside the frequency range of interest.

The structure is assumed to be at rest at the beginning of each loading. An initial transient in the structural response is therefore induced before the response becomes fully developed. This transient must be eliminated to ensure the proper response statistics are recovered. In the linear case, a moving block average of $1.0s$ of data was used to ascertain the point in the record at which the RMS displacement response became stable. In this manner, it was determined that elimination of the first $1.0s$ of the $2.0s$ record was more than sufficient. While the same criterion does not strictly apply to the nonlinear response case because of the dependence of the response on the initial conditions, it was employed with satisfactory results.
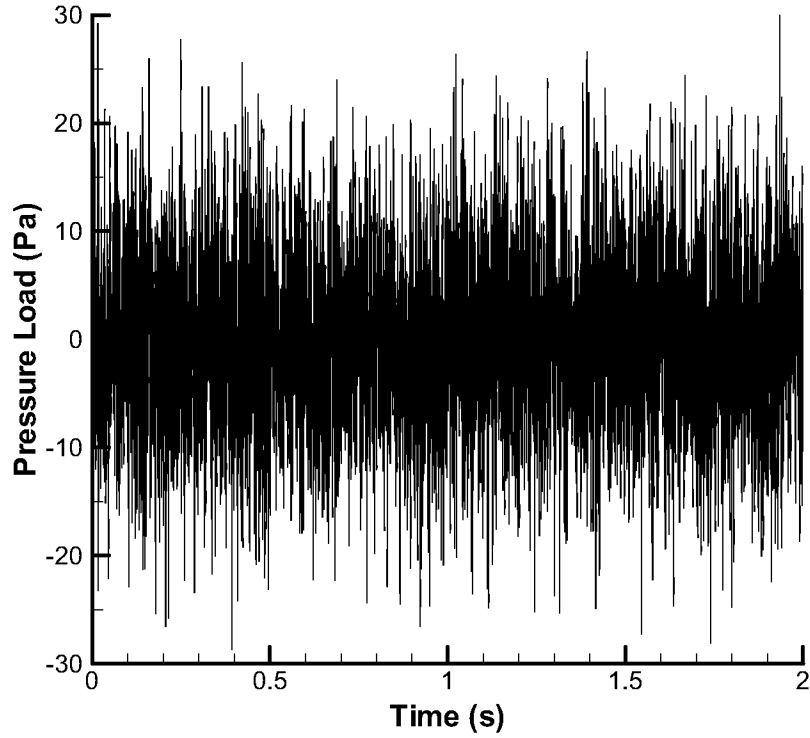
Figure 1: Typical acoustic loading time history.
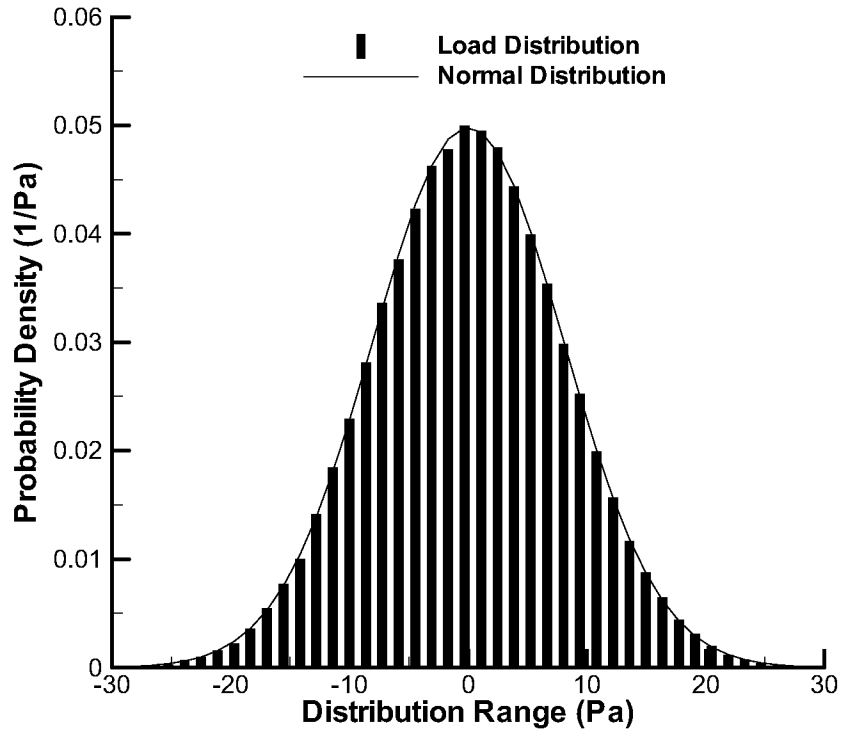
Figure 2: Typical probability density of acoustic loading.
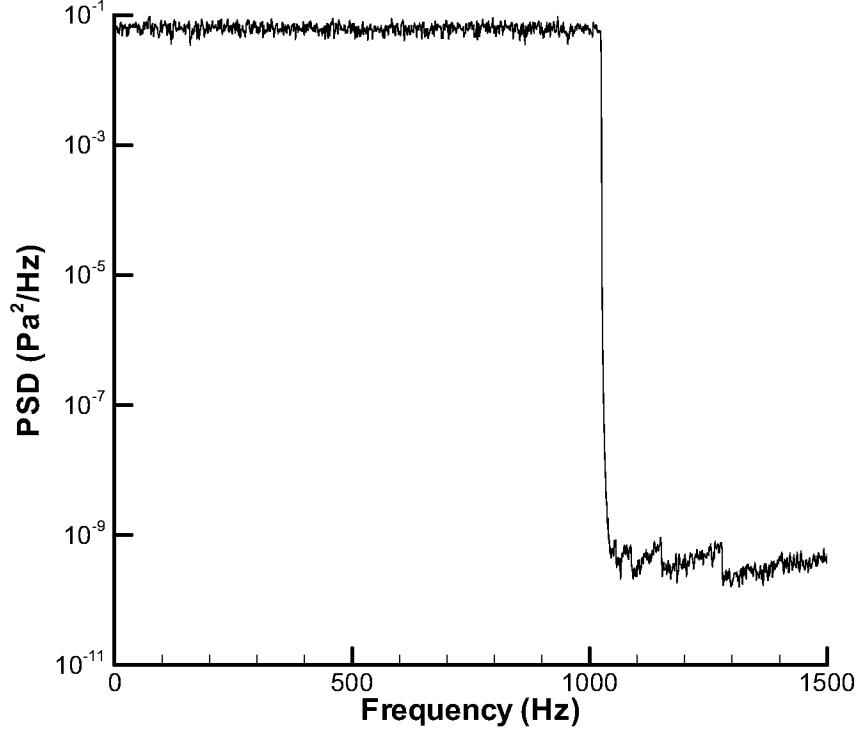
Figure 3: Typical averaged power spectral density of acoustic loading.

6.2. RESPONSE STATISTICS

Response statistics were generated from an ensemble of N=10 time histories at each load level. Estimates of the displacement RMS served as the basis for comparison with the EL method. Additionally, confidence intervals for the mean value of the displacement RMS estimate were generated to quantify the degree of uncertainty in the estimate [17] using:

$$\left[\bar{x} - \frac{st_{n;\square/n}}{\sqrt{N}} \leq \square_x \leq \bar{x} + \frac{st_{n;\square/n}}{\sqrt{N}} \right], \qquad n = N - 1 \tag{33}$$

where $\bar{x}$ and s^2 are the sample mean and variance of the RMS estimates from N ensembles, and t_n is the Student t distribution with n degrees of freedom, evaluated at $\square / 2$. For the 90% confidence intervals calculated, $\square = 0.1$.

Estimates of the displacement mean, skewness, and kurtosis were also computed to help ascertain the degree to which the assumptions made in the development of the EL method were followed. Power spectral density and probability density functions (PDF) of the displacement were computed for similar purposes.

16

7. RESULTS

Validation studies were conducted using a rectangular aluminum plate measuring 0.254m x 0.3556m of thickness, h, 0.00102m. All sides were simply supported. The material properties used were:

$$E \Box 7.3 \Box 10^{10} Pa, \qquad v \Box 0.3, \qquad \rho \Box 2763 \frac{kg}{m^3}$$

where E is the elastic modulus, v is Poisson's ratio, and ρ is the mass density. The plate was subjected to a spatially-uniform pressure loading over a computational bandwidth of 1024 Hz, as shown in Figure 1. Since the loading was uniformly distributed, only symmetric modes were included in the analysis. In general, any combination of symmetric and non-symmetric modes may be included.

A NASTRAN model of the full plate was built with 560 CQUAD4 elements measuring 0.0127m square for use in the EL analysis. The first two symmetric modes (modes 1 and 4) of this model had natural frequencies of 58.38 and 217.27 Hz. For comparison, the natural frequencies given by an analytical solution [18] were 58.34 and 216.01 Hz for the first two symmetric modes. These two modes were selected as participating modes in the EL and numerical simulation analyses. Modal damping was chosen to be sufficiently high (2.0% and 0.54% critical damping) so that a good comparison with the numerical simulation results could be made at the peaks of the PSD. The finite element model used in the numerical simulation analysis had the same element size (0.0127m square) as the NASTRAN model, but a quarter-plate model was used to reduce computational time. This model gave natural frequencies of 58.12 and 215.19 Hz for the first two symmetric plate modes. Both EL and simulation finite element models were checked for convergence by running additional analyses with models consisting of 0.00635m elements.

Analysis was performed at overall sound pressure levels from roughly 106 dB (4 Pa RMS) to roughly 160 dB (2048 Pa RMS), in 6 dB increments, giving a dynamic range of 54 dB. Figure 4 shows the normalized RMS out-of-plane (w) deflection at the plate center as a function of loading. Both force-error and potential energy-error minimization implementations are shown. The numerical simulation results are shown with 90% confidence intervals of the RMS estimate. At the lowest load level of 106 dB, the response is linear as can be seen by the comparison with

17

results from a strictly linear analysis (NASTRAN solution 111). Small, but noticeable, differences between the linear and nonlinear responses are noted at the 118 dB load level. The degree of nonlinearity increases with load level, as expected. At the highest level of 160 dB, the nonlinear response calculations predict RMS center deflections of 2.20 and 2.27 times the thickness for the force and potential energy-error minimization approaches, respectively. The 90% confidence interval on the numerical simulation data by comparison is $2.24 \leq w_{RMS}/h \leq 2.39$ at 160 dB. Consistent with past observations [11, 12], potential energy-error minimization results are closer to known solutions and somewhat higher (by a few percent) than force-error minimization results. The linear analysis by comparison predicts center deflections of nearly 13 times the thickness.
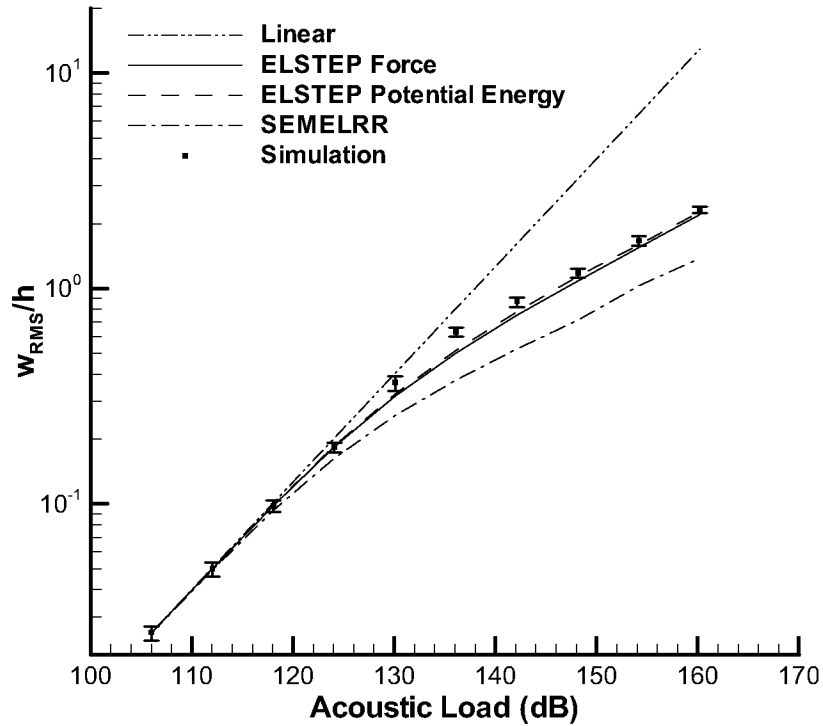
Figure 4: Normalized RMS center deflection as a function of acoustic load.

Results from the earlier SEMELRR implementation [9], also shown in Figure 4, were generated with the same NASTRAN model. These results are shown to significantly over-predict the effect of nonlinearity at loads as low as 124 dB. At 160 dB, the SEMELRR implementation predicts an RMS center deflection of 1.38 times the thickness, or approximately 60% less than

the mean of the numerical simulation prediction. The highly non-conservative nature of the SEMELRR analysis makes it unsuitable for nonlinear structural design.

In order to gain greater insight into the nonlinear dynamics, plots of the time history, PDF, and PSD are shown for three load levels, (106, 136 and 160 dB) in the following series of figures. Data in the time history and PDF plots correspond solely to numerical simulation results. Data in the PSD plots correspond to numerical simulation and EL results, where the EL results were generated by running a linear analysis (NASTRAN solution 111) using the modal equivalent linear stiffness K_e generated by the EL process previously described.

Results for the 106 dB excitation level are shown in Figure 5 – Figure 7. This excitation level was shown (see Figure 4) to produce a linear response. As expected, the PDF mimics the normally distributed PDF of the input shown in Figure 1. The averaged PSD shows excellent agreement between the EL, linear, and numerical simulation results. This agreement helps to establish the confidence in making comparisons between these two fundamentally different analyses.
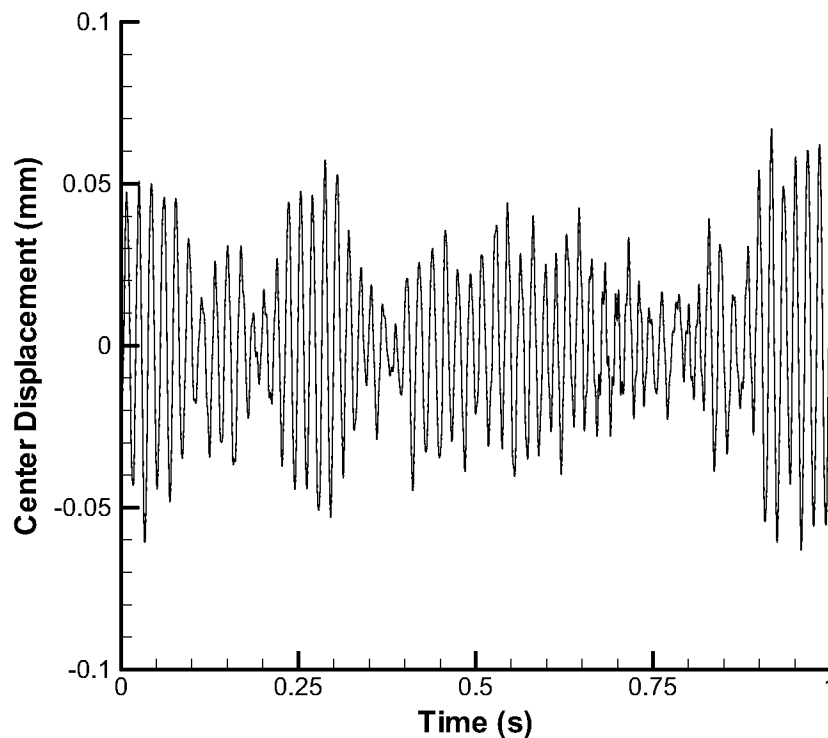
Figure 5: Time history of center displacement response at 106 dB.

19
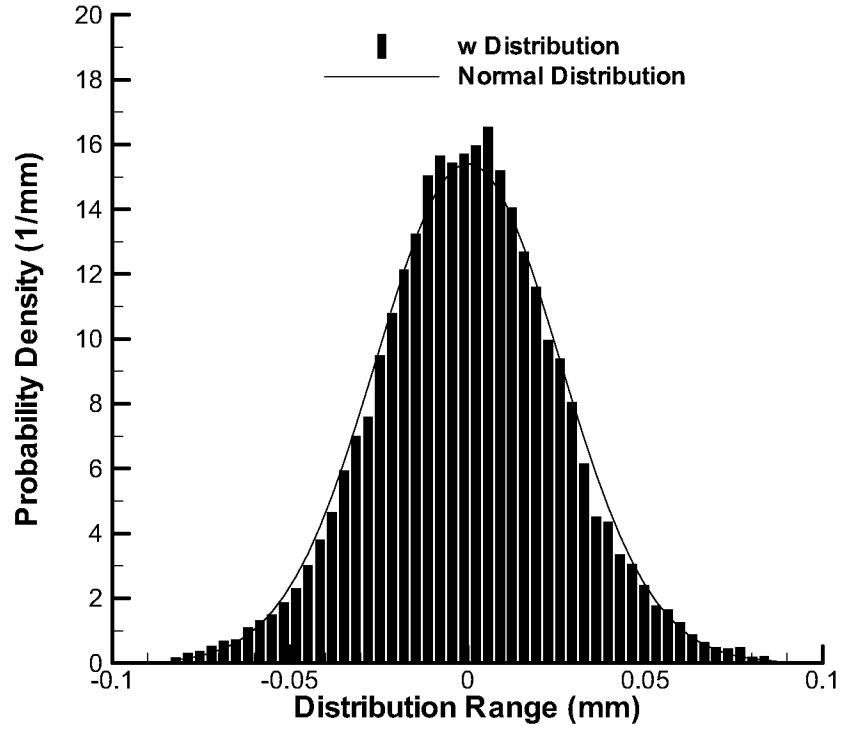
Figure 6: Probability density of center displacement response at 106 dB.
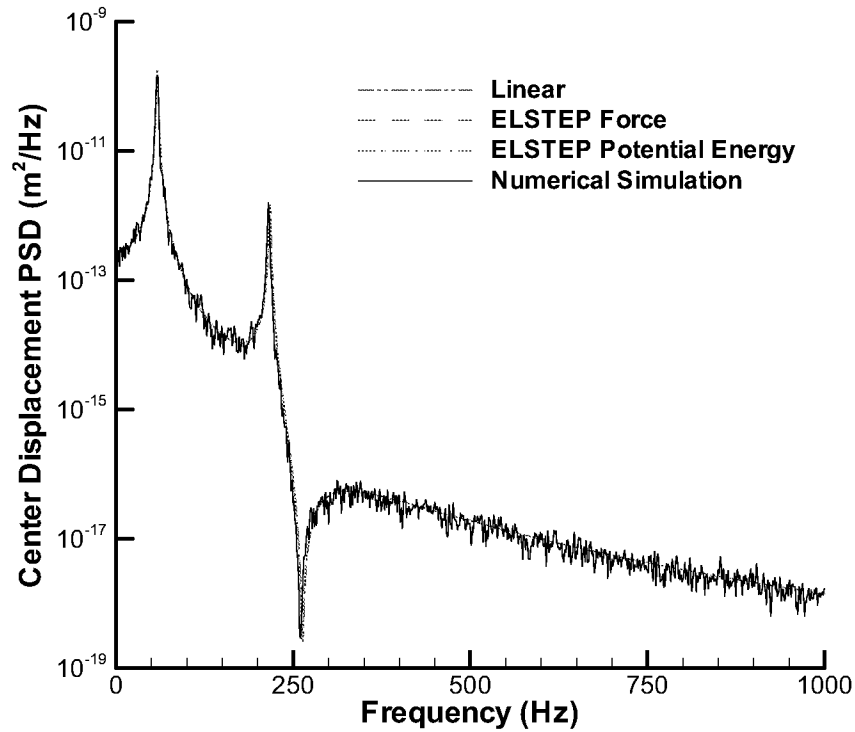
Figure 7: Power spectral density of center displacement response at 106 dB.

20

Figure 8 – Figure 10 show the nonlinear response associated with the 136 dB excitation level. The time history of the center displacement has a visibly higher peak probability and the PDF exhibits a minor flattening at the peak. The shapes of the PSDs from the EL analyses are those of the equivalent linear systems. Thus, the PSDs from the EL analyses do not show the peak broadening effect observed in the numerical simulation. Additionally, harmonics in the structural response are present only in the numerical simulation results. The PSDs from both the numerical simulation and EL analyses show a positive shift in the frequency of the fundamental mode compared with the linear solution. Both EL analyses shift the fundamental frequency by nominally the same amount and fall within the broadening fundamental peak of the numerical simulation analysis. The frequency of the second mode from the force-error minimization analysis also increases and more closely matches the numerical simulation data than does the potential energy-error minimization analysis, which shows a negative frequency shift.
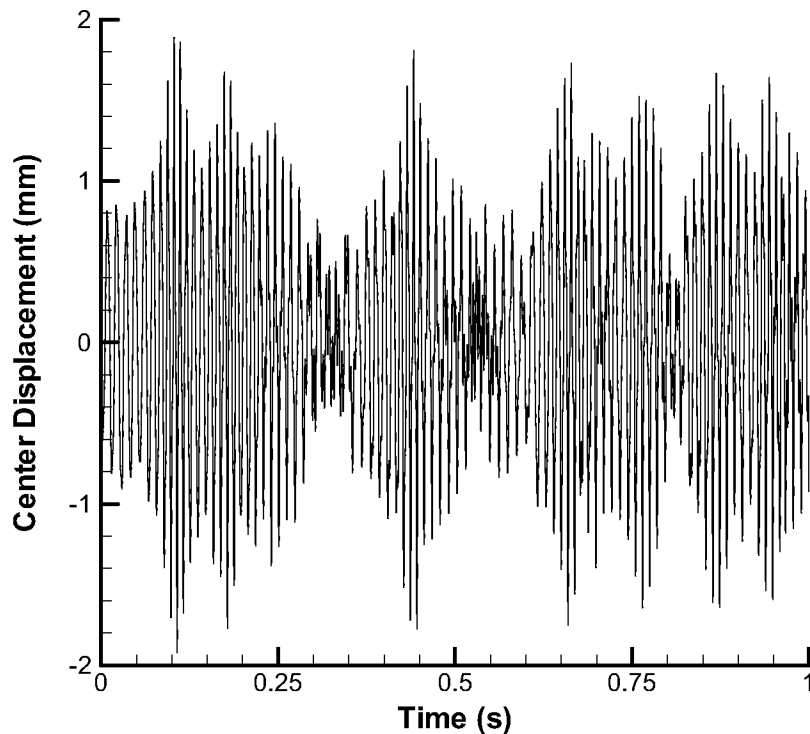
Figure 8: Time history of center displacement response at 136 dB.

21
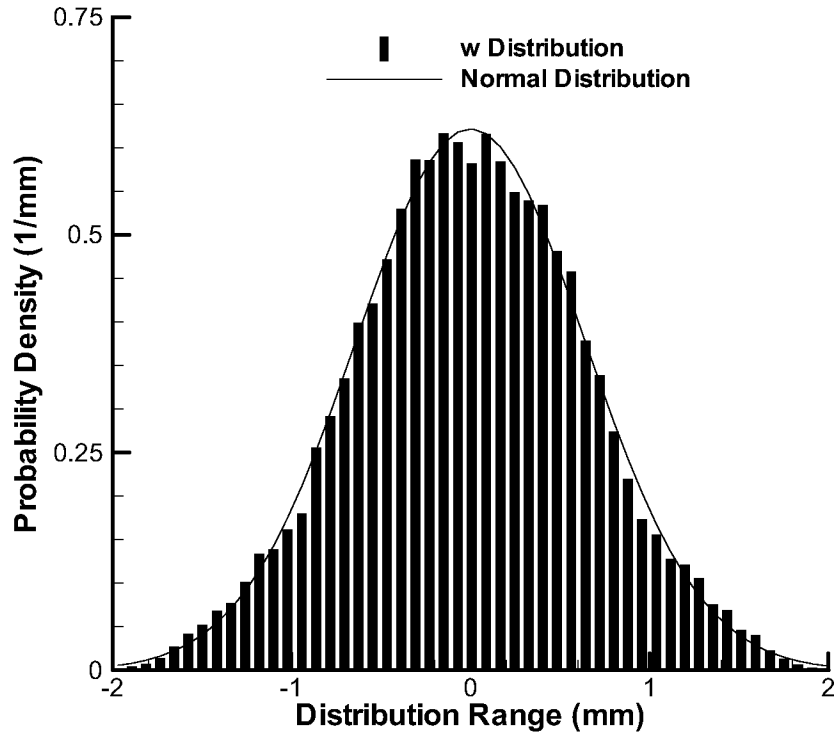
Figure 9: Probability density of center displacement response at 136 dB.
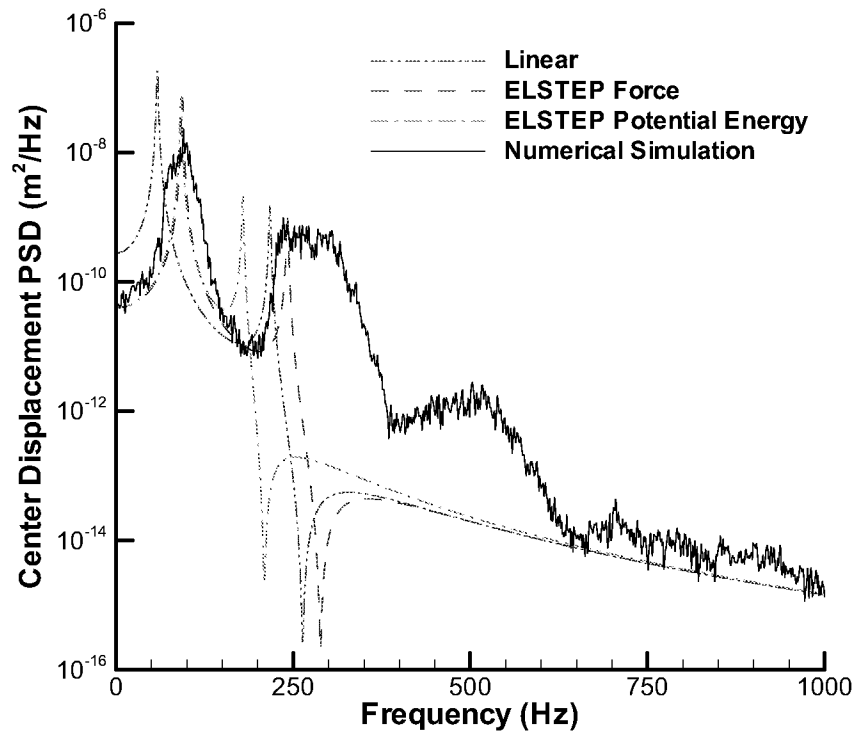
Figure 10: Power spectral density of center displacement response at 136 dB.

To investigate this behavior further, the fundamental and second mode frequencies as a function of applied load are shown in Figure 11. The shift in the frequency of the fundamental mode is consistently positive and close in value between the force and potential energy EL analyses. The shift in second mode frequency differs between the two EL analyses, with the force EL results showing similar behavior to the fundamental, while the potential energy EL results first displaying a drop, then an increase in frequency with increasing load. Since the force-error minimization approach fully takes into account the internal force resulting from bending-membrane coupling, this approach gives results that are consistent with numerical simulation results. The potential energy-error minimization approach places no demand on the internal force. Since most of the strain energy in this case is associated with the fundamental mode, that behavior is accurately captured. The second mode, having significantly less potential energy, is allowed to shift without constraint.
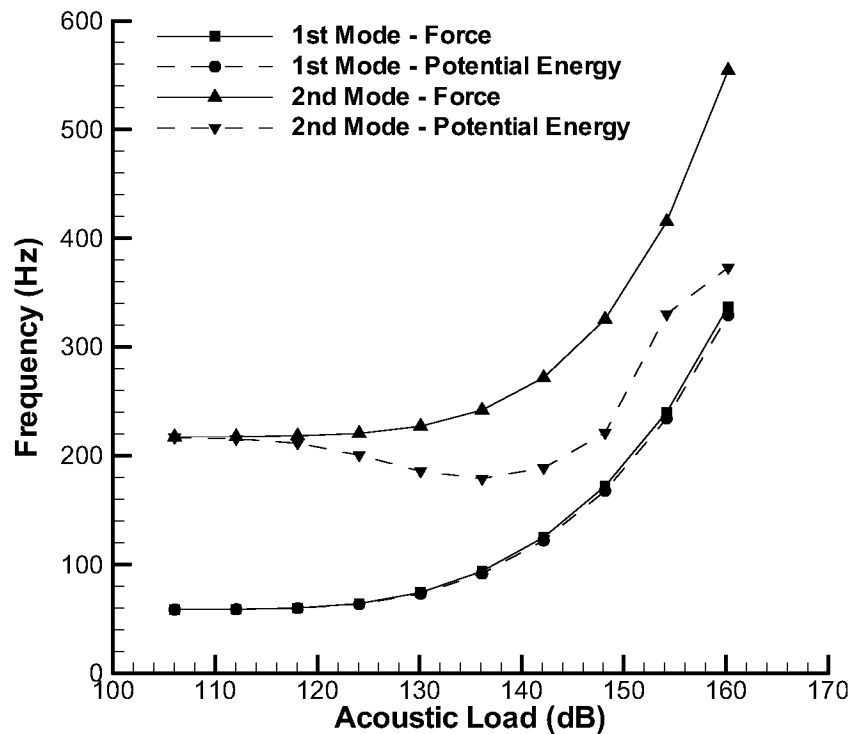
Figure 11: Shift in fundamental and second mode frequencies as a function of applied load for both EL analyses.

While this behavior appears inconsistent, recall that both EL approaches minimize the error between the equivalent linear and nonlinear systems through the modal equivalent stiffness

23

matrix $\boldsymbol{K}_e$, which is a function of the modal displacement. It is therefore expected that only the RMS displacement, or the area under the displacement PSD, should be the same between either EL analysis and the numerical simulation analysis, and not the shape of the PSD itself. This is consistent with the observations.

The highest degree of nonlinearity is shown in Figure 12 – Figure 14, corresponding to a 160 dB acoustic load. The time history is further peak oriented and the PDF exhibits substantial flattening. The peak broadening in the PSD of the numerical simulation results is severe, and nearly flattens the spectrum above 350 Hz. With regard to the EL analyses, positive shifts in the frequencies of the fundamental mode are comparable between the two EL analyses. Shifts in the second mode frequencies are more substantial in the force-error minimization approach than in the potential energy-error minimization.
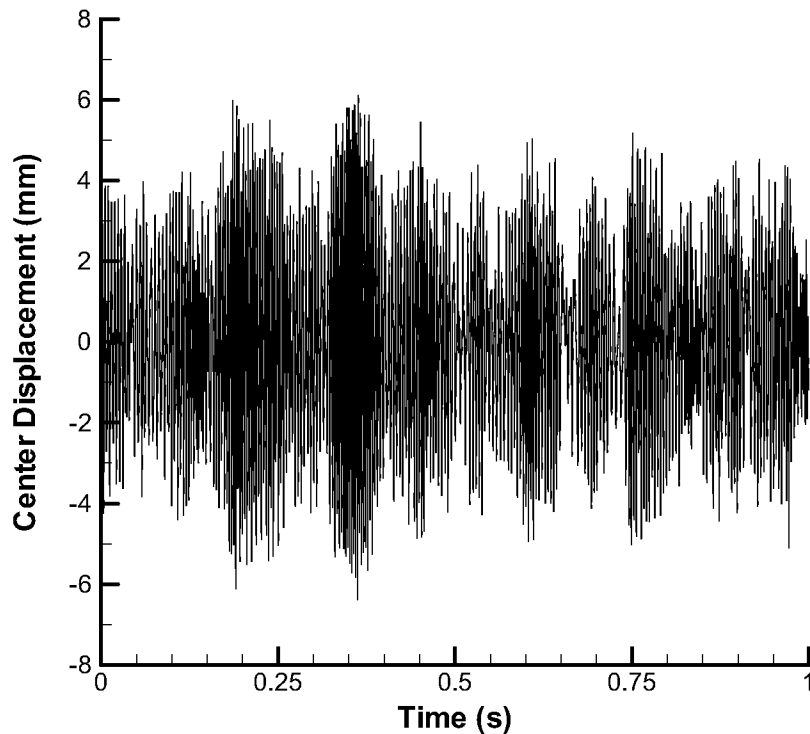
Figure 12: Time history of center displacement response at 160 dB.
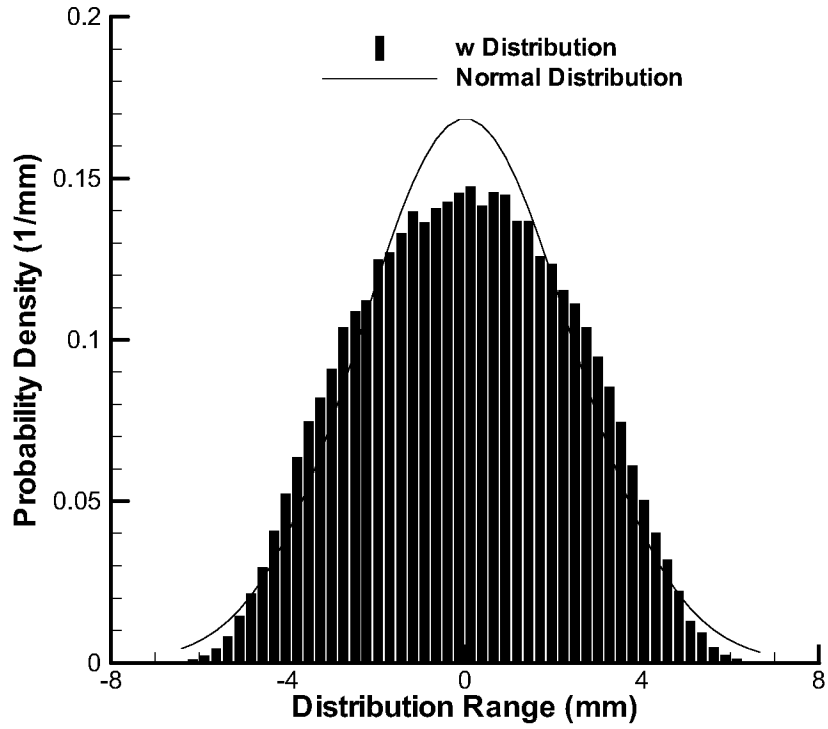
Figure 13: Probability density of center deflection response at 160 dB.
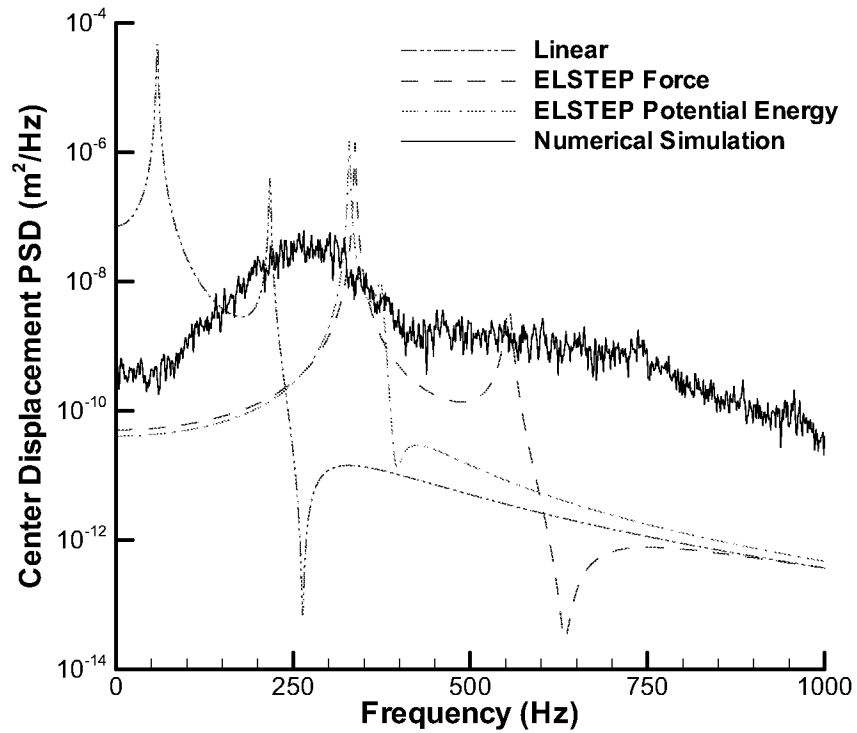
Figure 14: Power spectral density of center deflection response at 160 dB.

Moments of the center displacement were calculated from the numerical simulation results for all load levels. They are provided in Table 1 with the RMS center displacement from both EL analyses. The EL and numerical simulation results agree well, thus validating the EL analysis over a substantial load range. The validity of assumptions made in the development of the EL method is ascertained by observing the mean, skewness and kurtosis. The mean value is effectively zero for all load levels, indicating the assumption of zero mean response has not been violated. Although the PDF is more or less skew-symmetric, the shape is flattened at the higher load levels as indicated by a decreasing kurtosis from the linear value of 3. The decreasing kurtosis values indicate a violation of the Gaussian response assumption. However, even with this non-Gaussian response distribution, the EL analyses give good predictions of the RMS response.

Plots of the RMS displacement over the entire plate are shown in Figure 15 – Figure 17 for the linear and EL analyses for the 160 dB load case. While the plots appear similar in character, the linear displacement contours look rounder than those of the two EL analyses. To better understand the nature of these differences, the RMS displacements were normalized with respect to their maximum (center) displacement for each of the three cases. The differences between the normalized linear and force-error minimization EL displacements, and the normalized linear and potential energy-error minimization EL displacements are shown in Figure 18 – Figure 19. These are expressed in percent with respect to the maximum normalized displacement (unity). In each case, the greatest difference occurs along the horizontal centerline and near the short sides of the plate. These plots highlight the need to perform a nonlinear analysis to obtain the proper spatial distribution. As previously noted, the difference between the two EL analyses is small relative to their displacement, as shown in Figure 20. The difference resembles the second symmetric mode. This observation is consistent with the PSD in Figure 14, which indicates the maximum magnitude difference between the two EL analyses to be associated with the second mode.

Table 1: Moments of the center displacement.

Load (dB)	Force Error EL RMS (m)	Potential Energy Error EL RMS (m)	SEMELRR RMS (m)	Num Sim Mean (m)	Numerical Simulation RMS (m) (90% Confidence Interval)	Skewness	Kurtosis
106	2.57×10^{-5}	2.57×10^{-5}	2.56×10^{-5}	$+1.56 \times 10^{-7}$	2.37×10^{-5} RMS $< 2.76 \times 10^{-5}$	$+0.0017$	3.21
112	5.12×10^{-5}	5.12×10^{-5}	5.04×10^{-5}	$+3.07 \times 10^{-7}$	4.68×10^{-5} RMS $< 5.47 \times 10^{-5}$	$+0.0013$	3.18
118	1.00×10^{-4}	1.01×10^{-4}	9.54×10^{-5}	$+1.01 \times 10^{-8}$	9.34×10^{-5} RMS $< 1.06 \times 10^{-4}$	$+0.0012$	2.90
124	1.88×10^{-4}	1.90×10^{-4}	1.66×10^{-4}	$+7.94 \times 10^{-7}$	1.76×10^{-4} RMS $< 1.96 \times 10^{-4}$	$+0.0027$	2.60
130	3.24×10^{-4}	3.30×10^{-4}	2.62×10^{-4}	$+1.87 \times 10^{-6}$	3.42×10^{-4} RMS $< 4.01 \times 10^{-4}$	-0.0010	2.81
136	5.13×10^{-4}	5.27×10^{-4}	3.84×10^{-4}	-5.23×10^{-7}	6.09×10^{-4} RMS $< 6.71 \times 10^{-4}$	$+0.0033$	2.83
142	7.68×10^{-4}	7.95×10^{-4}	5.35×10^{-4}	-3.18×10^{-7}	8.38×10^{-4} RMS $< 9.30 \times 10^{-4}$	$+0.0032$	2.48
148	1.10×10^{-3}	1.16×10^{-3}	7.27×10^{-4}	$+2.58 \times 10^{-6}$	1.14×10^{-3} RMS $< 1.26 \times 10^{-3}$	-0.0063	2.38
154	1.58×10^{-3}	1.63×10^{-3}	1.05×10^{-3}	$+1.04 \times 10^{-6}$	1.61×10^{-3} RMS $< 1.79 \times 10^{-3}$	$+0.0012$	2.36
160	2.25×10^{-3}	2.32×10^{-3}	1.41×10^{-3}	$+6.05 \times 10^{-6}$	2.29×10^{-3} RMS $< 2.44 \times 10^{-3}$	-0.0061	2.28

RMS Disp (m)

	1.32E-02
	1.22E-02
	1.13E-02
	1.04E-02
	9.41E-03
	8.47E-03
	7.53E-03
	6.59E-03
	5.65E-03
	4.71E-03
	3.76E-03
	2.82E-03
	1.88E-03
	9.41E-04
	0.00E+00
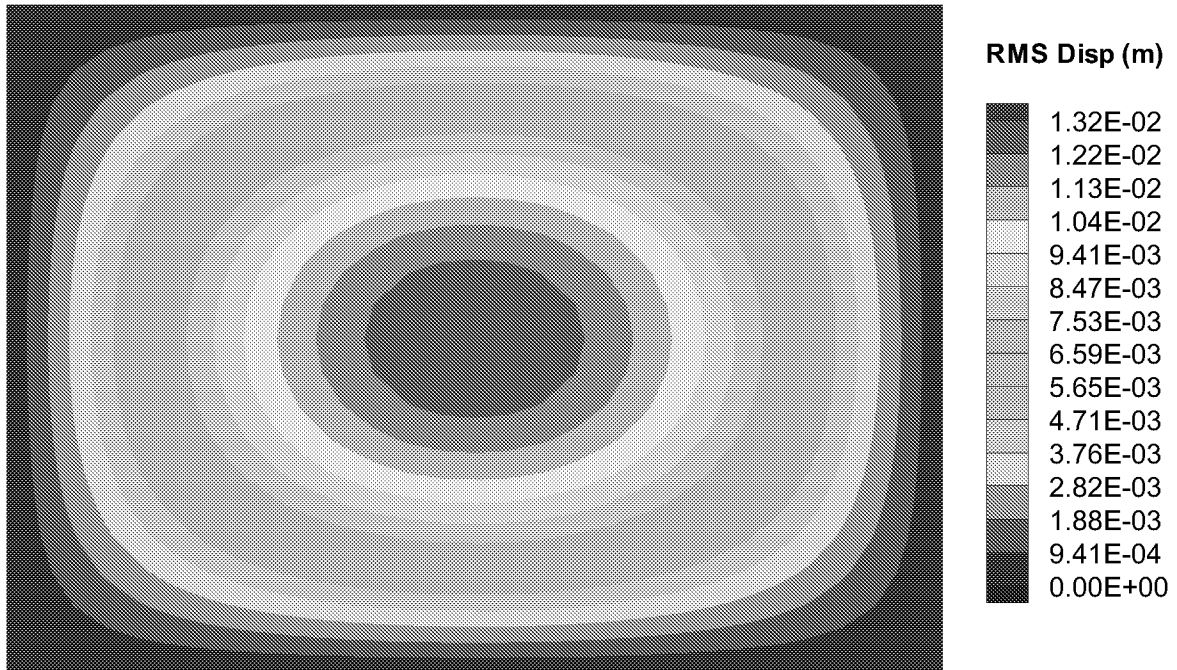
Figure 15: Contour plot of RMS displacement from linear analysis at 160 dB.

RMS Disp (m)

	2.30E-03
	2.14E-03
	1.97E-03
	1.81E-03
	1.64E-03
	1.48E-03
	1.31E-03
	1.15E-03
	9.86E-04
	8.21E-04
	6.57E-04
	4.93E-04
	3.29E-04
	1.64E-04
	0.00E+00
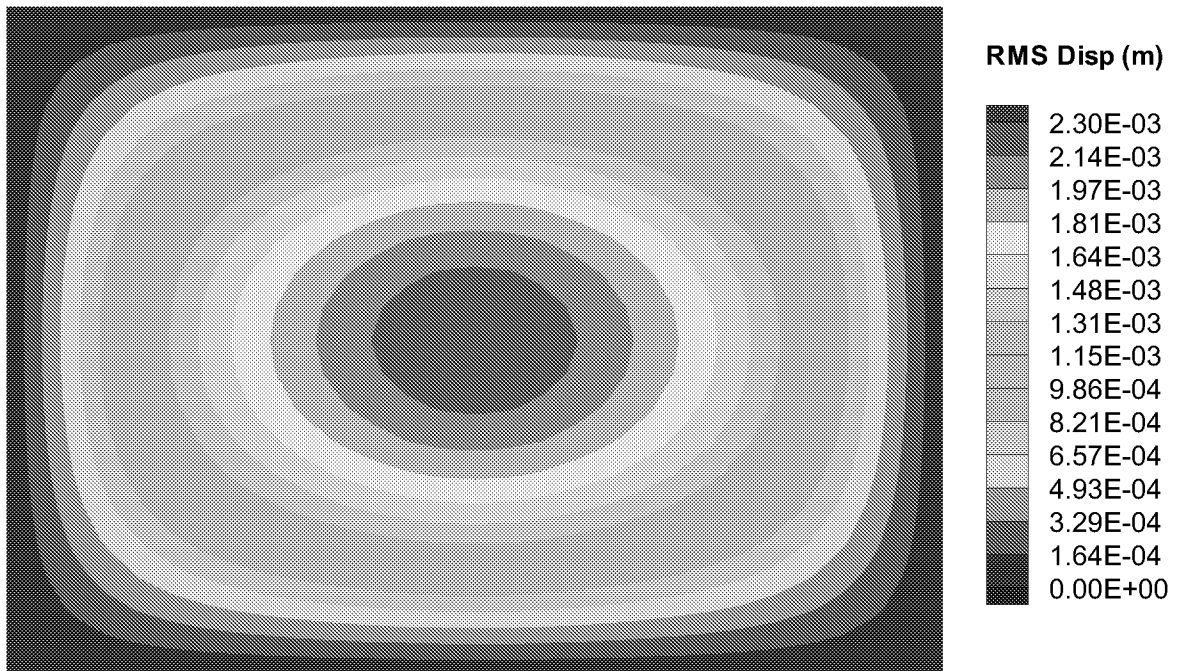
Figure 16: Contour plot of RMS displacement from force-error EL analysis at 160 dB.

28

RMS Disp (m)

	2.30E-03
	2.14E-03
	1.97E-03
	1.81E-03
	1.64E-03
	1.48E-03
	1.31E-03
	1.15E-03
	9.86E-04
	8.21E-04
	6.57E-04
	4.93E-04
	3.29E-04
	1.64E-04
	0.00E+00
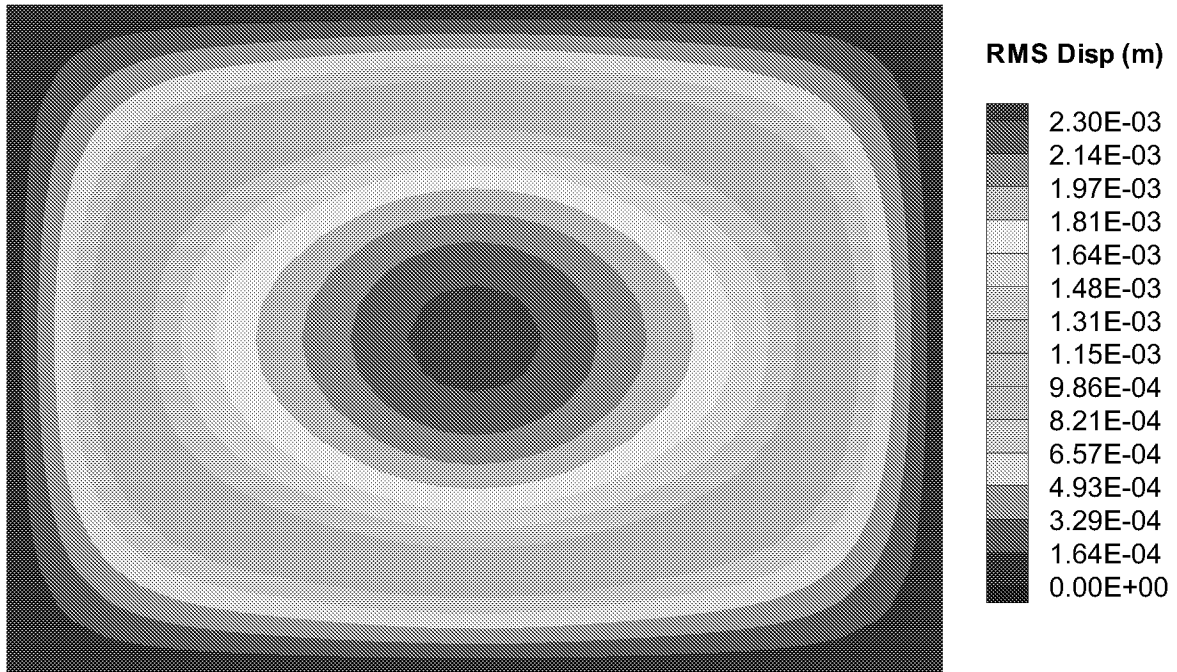
Figure 17: Contour plot of RMS displacement from potential energy-error EL analysis at 160 dB.

Percent RMS
Displacement
Difference

	5.40
	5.01
	4.62
	4.24
	3.85
	3.46
	3.07
	2.69
	2.30
	1.91
	1.52
	1.13
	0.75
	0.36
	-0.03
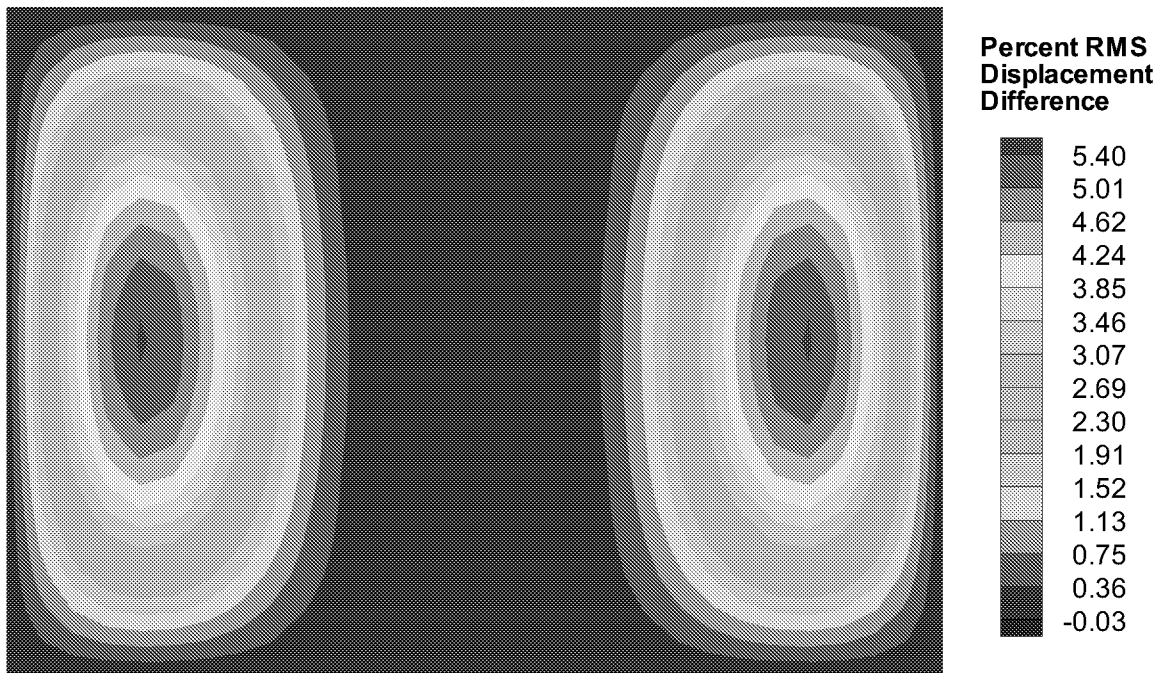
Figure 18: Difference between normalized linear and force-error EL displacements at 160 dB.

29
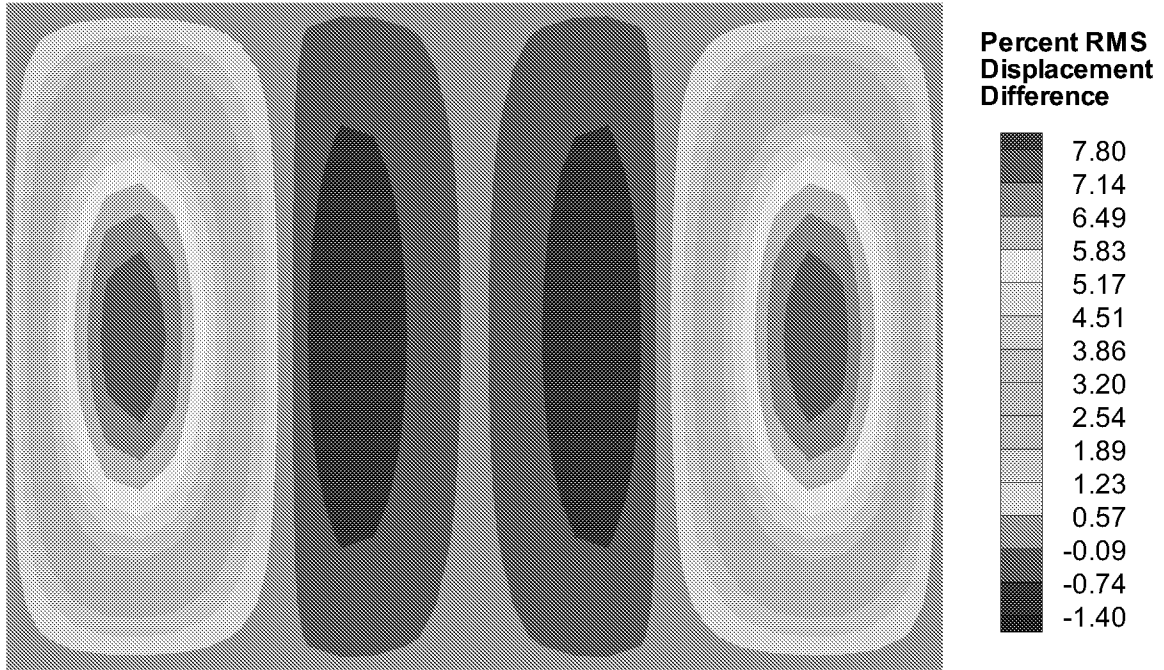
Figure 19: Difference between normalized linear and potential energy-error EL displacements at 160 dB.
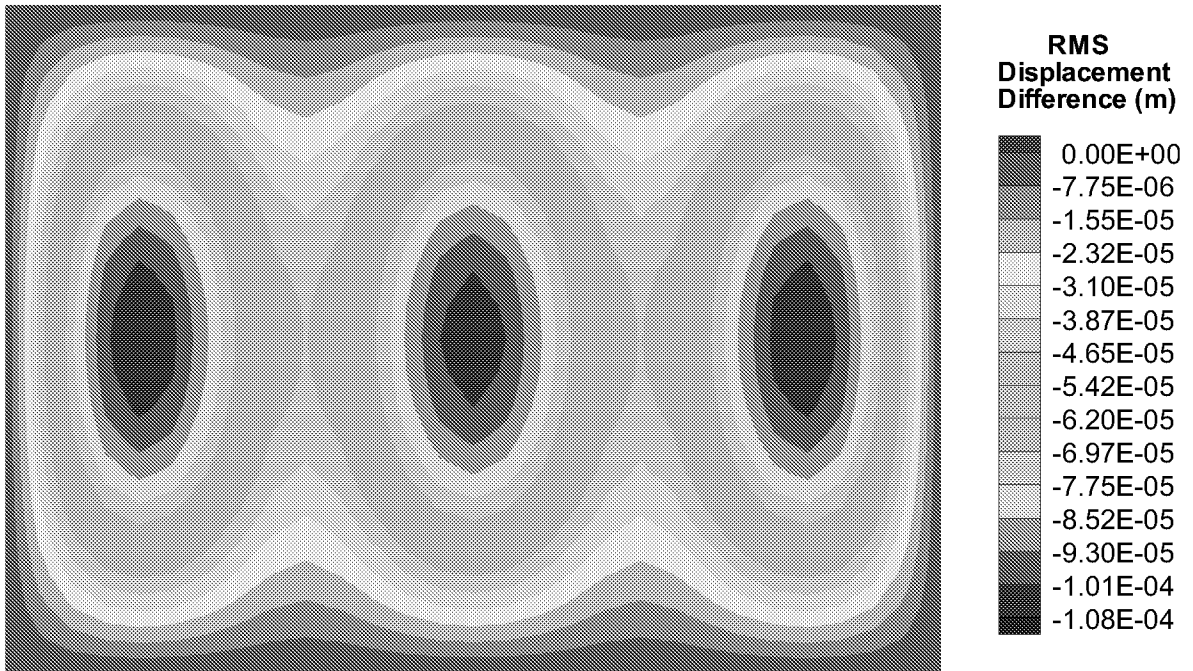
Figure 20: Difference between displacements from force-error and potential energy-error minimization analyses at 160 dB.

8. DISCUSSION

Differences between the two EL analyses and the numerical simulation do exist and warrant some discussion. It is seen that the EL approach slightly over-predicts the degree of nonlinearity compared to the numerical simulation results. Interestingly, the greatest differences appear in the moderately nonlinear regime. The differences do not appear to be due to a violation of the assumption of a Gaussian response because the over-prediction does not correlate with increasing kurtosis of response. The trends observed here are consistent with comparisons between a different numerical simulation analysis and a force-error minimization EL analysis of a clamped-clamped beam [13]. Comparisons of the force and potential energy-error minimization approaches with an F-P-K solution of a beam, however, indicate that EL solutions span the exact solution, with the potential energy-error minimization results being slightly higher and the force-error minimization results being slightly lower than the exact solution [12]. It would therefore appear that the numerical simulation solutions are less stiff than the EL solutions in the moderately nonlinear regime, but this has yet to be fully substantiated.

Some implications on the use of the EL technique as a basis for fatigue life calculations are worth mentioning. First, assuming that stresses or strains from the EL technique will compare equally well with those from the numerical simulation analysis, a simple fatigue-life calculation based on RMS levels will be much less conservative than calculations based on linear analyses. This offers the potential for substantial weight savings for structures designed using nonlinear methods. Secondly, it appears that a nonlinear analysis, EL or otherwise, is required to accurately calculate the RMS deflected shape. Use of a linear RMS deflected shape scaled to the nonlinear level would inaccurately reflect the spatial distribution. Simple fatigue-life calculations based on the RMS stress or strain could be significantly affected as these quantities depend on the spatial distribution of the deformation. Lastly, use of the EL-derived PSD response in a more sophisticated fatigue-life calculation requires careful investigation. Recall that peaks in the equivalent linear PSD may occur at different frequencies than in the PSD from the numerical simulation analysis, as shown in Figure 10 and Figure 14. Methods such as spectral fatigue analysis [19], which take moments of the PSD, may incorrectly account for the contribution of a particular frequency component in the cycle counting scheme. It is not known, for example, if the narrowly shaped, higher fundamental frequencies of the equivalent linear PSD result in

31

conservative or non-conservative estimates of fatigue life relative to predictions made using the numerical simulation PSD with more broadly shaped, lower fundamental frequencies. An assessment of this effect is left as an area for further study.

9. CONCLUSIONS

A novel method for determining nonlinear stiffness coefficients of arbitrary structures has been developed. The method can be implemented in any finite element code having a geometrically nonlinear static capability. It has been implemented as a DMAP alter to MSC.NASTRAN to demonstrate its effectiveness.

A potential energy-error minimization EL approach has been extended to handle multiple degree-of-freedom systems. The RMS random response predictions from it and the traditional force-error minimization approach have been validated through comparison with a numerical simulation method over a wide range of load levels. Comparisons with numerical simulation results are good, even when the assumption of Gaussian response has been violated. It has been shown that a linear analysis grossly over-predicts the RMS displacements (i.e., it is too conservative) in comparison with numerical simulation results. The potential energy-error minimization approach provided a slightly more conservative estimate of RMS displacement than the force-error minimization approach. It was demonstrated that an earlier EL implementation (SEMELRR) significantly over-predicts the effect of nonlinearity (i.e., it is non-conservative).

ACKNOWLEDGEMENTS

REFERENCES

[1]   Bolotin, V.V., *Statistical methods in structural mechanics*, Holden-Day, Inc., 1969.

[2]   Lin, Y.K., *Probabilistic Theory of Structural Dynamics*. Malabar, FL, R.E. Krieger, 1976.

[3]   Caughy, T.K., "Equivalent linearization techniques," *Journal of the Acoustical Society of America*, Vol. 35, pp. 1706-1711, 1963.

[4]   Roberts, J.B. and Spanos, P.D., *Random vibration and statistical linearization*. New York, NY, John Wiley & Sons, 1990.

[5]   Atalik, T.S. and Utku, S., "Stochastic linearization of multi-degree-of-freedom nonlinear systems," *Earthquake engineering and structural dynamics*, Vol. 4, pp. 411-420, 1976.

[6]   Elishakoff, I. and Zhang, R., "Comparison of new energy-based versions of the stochastic linearization technique," *IUTAM Symposium*, Springer-Verlag, pp. 201-211, Turin, 1992.

[7]   Fang, J. and Elishakoff, I., "Nonlinear response of a beam under stationary excitation by improved stochastic linearization method," *Applied Mathematical Modelling*, Vol. 19, pp. 106-111, 1995.

[8]   Chiang, C.K., Mei, C. and Gray, C.E., "Finite element large-amplitude free and forced vibrations of rectangular thin composite plates," *Journal of Vibration and Acoustics*, Vol. 113, No. July, pp. 309-315., 1991.

[9]   Robinson, J.H., Chiang, C.K., and Rizzi, S.A., "Nonlinear Random Response Prediction Using MSC/NASTRAN," NASA TM-109029, October 1993.

[10]   "MSC/NASTRAN Quick Reference Guide, Version 70.5," MacNeal Schwendler Corporation, 1998.

[11]   Muravyov, A.A., Turner, T.L., Robinson, J.H., and Rizzi, S.A., "A New Stochastic Equivalent Linearization Implementation for Prediction of Geometrically Nonlinear Vibrations," *Proceedings of the 40th AIAA/ASME/ASCE/AHS/ASC Structures, Structural Dynamics and Materials Conference*, Vol. 2, AIAA-99-1376, pp. 1489-1497, St. Louis, MO, 1999.

[12]   Muravyov, A.A., "Determination of Nonlinear Stiffness Coefficients for Finite Element Models with Application to the Random Vibration Problem," *MSC Worldwide Aerospace Conference Proceedings*, MacNeal-Schwendler Corp., Vol. 2, pp. 1-14, Long Beach, 1999.

[13]   Rizzi, S.A. and Muravyov, A.A., "Comparison of Nonlinear Random Response Using Equivalent Linearization and Numerical Simulation," *Structural Dynamics: Recent Advances, Proceedings of the 7th International Conference*, Vol. 2, pp. 833-846, Southampton, England, 2000.

[14]   Mei, C., Dhainaut, J.M., Duan, B., Spottswood, S.M., and Wolfe, H.F., "Nonlinear Random Response of Composite Panels in an Elevated Thermal Environment," Air Force Research Laboratory, Wright-Patterson Air Force Base, OH, AFRL-VA-WP-TR-2000-3049, October 2000.

[15]   "MSC/NASTRAN Version 68 DMAP Module Dictionary," Bella, D. and Reymond, M., Eds., MacNeal-Schwendler Corporation, Los Angeles, CA, 1994.

[16]   Rizzi, S.A. and Muravyov, A.A., "Improved Equivalent Linearization Implementations Using Nonlinear Stiffness Evaluation," NASA TM-2001-210838, March 2001.

[17]   Bendat, J.S. and Piersol, A.G., *Random data: Analysis and measurement procedures*, Wiley-Interscience, 1971.

[18]   Leissa, A.W., "Vibration of Plates," NASA SP-160, 1969.

[19]   Bishop, N.W.M. and Sherratt, F., "A theoretical solution for the estimation of rainflow ranges from power spectral density data," *Fat. Fract. Engng. Mater. Struct.*, Vol. 13, pp. 311-326, 1990.

REPORT DOCUMENTATION PAGE

Public reporting burden for this collection of information is estimated to average 1 hour per response, including the time for reviewing instructions, searching existing data sources, gathering and maintaining the data needed, and completing and reviewing the collection of information. Send comments regarding this burden estimate or any other aspect of this collection of information, including suggestions for reducing this burden, to Washington Headquarters Services, Directorate for Information Operations and Reports, 1215 Jefferson Davis Highway, Suite 1204, Arlington, VA 22202-4302, and to the Office of Management and Budget, Paperwork Reduction Project (0704-0188), Washington, DC 20503.

1. AGENCY USE ONLY (Leave blank)	2. REPORT DATE	3. REPORT TYPE AND DATES COVERED
	July 2002	Technical Publication

4. TITLE AND SUBTITLE
Equivalent Linearization Analysis of Geometrically Nonlinear Random Vibrations Using Commercial Finite Element Codes

5. FUNDING NUMBERS
522-63-11-03

6. AUTHOR(S)
Stephen A. Rizzi
Alexander A. Muravyov

7. PERFORMING ORGANIZATION NAME(S) AND ADDRESS(ES)
NASA Langley Research Center
Hampton, VA 23681-2199

8. PERFORMING ORGANIZATION REPORT NUMBER
L-18219

9. SPONSORING/MONITORING AGENCY NAME(S) AND ADDRESS(ES)
National Aeronautics and Space Administration
Washington, DC 20546-0001

10. SPONSORING/MONITORING AGENCY REPORT NUMBER
NASA/TP-2002-211761

12a. DISTRIBUTION/AVAILABILITY STATEMENT
Unclassified-Unlimited
Subject Category 39   Distribution: Standard
Availability: NASA CASI (301) 621-0390

12b. DISTRIBUTION CODE

13. ABSTRACT (Maximum 200 words)
Two new equivalent linearization implementations for geometrically nonlinear random vibrations are presented. Both implementations are based upon a novel approach for evaluating the nonlinear stiffness within commercial finite element codes and are suitable for use with any finite element code having geometrically nonlinear static analysis capabilities. The formulation includes a traditional force-error minimization approach and a relatively new version of a potential energy-error minimization approach, which has been generalized for multiple degree-of-freedom systems. Results for a simply supported plate under random acoustic excitation are presented and comparisons of the displacement root-mean-square values and power spectral densities are made with results from a nonlinear time domain numerical simulation.

14. SUBJECT TERMS
Geometrically nonlinear random vibration, equivalent linearization, statistical linearization, force error minimization, potential energy error minimization, sonic fatigue, nonlinear stiffness

15. NUMBER OF PAGES
39

16. PRICE CODE

17. SECURITY CLASSIFICATION OF REPORT	18. SECURITY CLASSIFICATION OF THIS PAGE	19. SECURITY CLASSIFICATION OF ABSTRACT	20. LIMITATION OF ABSTRACT
Unclassified	Unclassified	Unclassified	UL

NSN 7540-01-280-5500

Standard Form 298 (Rev. 2-89)
Prescribed by ANSI Std. Z-39-18
298-102